3DRA Reconstruction of Intracranial Aneurysms – How does Voxel Size Influences Morphologic and Hemodynamic Parameters*

Philipp Berg, Livia Radtke, Samuel Voß, Steffen Serowy, Gábor Janiga, Berhard Preim, Oliver Beuing, Sylvia Saalfeld

Abstract— **Three-dimensional shape analysis and image-based hemodynamic simulations are widely used to assess the individual rupture risk of intracranial aneurysms. However, the quality of those results highly depends on pre-simulative working steps including image reconstruction and segmentation.**

Within this study, three patient-specific aneurysms were reconstructed using three different voxel sizes (0.1 mm, 0.3 mm, 0.5 mm). Afterwards, 3D segmentations and time-dependent blood flow simulations were carried out to evaluate the impact of the reconstruction size.

The results indicate that overall all voxel sizes lead to a qualitatively good agreement with respect to the aneurysm surfaces. However, deviations occur regarding the neck representation as well as the consideration of perforating arteries. Further, morphological differences lead to clear hemodynamic variations, especially for shear force predictions.

The findings indicate that depending on the desired analysis, careful reconstruction parameter selection is required. Particularly, for quantitative morphology and blood flow studies, the early step of reconstruction can have a crucial effect on subsequent results.

I. Introduction

Intracranial aneurysms are permanent malformations of the cerebral vasculature and occur at several locations of the Circle of Willis [1]. Since aneurysms can completely differ with respect to their phenotype as well as the hemodynamic situation, individualized therapy is required. To assess the rupture risk or support the treatment planning of intracranial aneurysms, hemodynamic simulations are increasingly applied. However, due to several simplifications and the lack of patient-specific boundary conditions (e.g., individual flow rates), clinical acceptance remains limited. In order to improve this situation, influences that impact the quality of image-based simulations need to be analyzed and respected in subsequent research studies.

It has been demonstrated by Valen-Sendstad et al. [2] that the correct geometric representation of an aneurysm has a primary effect, while for instance outlet boundary conditions or the treatment of blood as a Newtonian fluid have only secondary influence [3, 4]. Additionally, the variability of numerical methods for cerebral simulations was extensive evaluated [5]. However, in order to provide an appropriate virtual vasculature, careful reconstruction and segmentation need to be carried out. In this regard, Berg et al. [6] revealed the impact of different reconstruction kernels on morphologic and hemodynamic results. Furthermore, Lauric et al. [7] found that the choice of angiographic modality as well as the reconstruction kernel has a critical impact on aneurysm morphology and blood flow results.

Hence, this study is an important extension to the previous works, since it focuses on the effect of reconstruction voxel size. Here, three intracranial aneurysms were chosen and reconstructed with three different voxel sizes. Therefore, nine cases were evaluated with respect to morphologic and hemodynamic differences. This allows for recommendations regarding the reconstruction, if quantitative blood flow studies are desired and enables research groups to carefully select their reconstruction settings in advance.

II. Materials and Methods

A. Case Description

Within this study, three randomly selected patient-specific aneurysms were included. These were located at the internal carotid artery (Case 1), anterior communicating artery (Case2) and middle cerebral artery (Case 3), respectively. All patients were minimal-invasively treated using either stent-assisted coiling or flow diverter placement.

B. Reconstructions

The raw 3D rotational angiography (3DRA) images of each dataset were reconstructed using three different resolutions on an Artis Q angiography system (Siemens Healthineers, Forchheim, Germany). These comprise the resolutions “small” (Δx_s = 0.1 mm), “medium” (Δx_m = 0.3 mm) and “full” (Δx_f = 0.5 mm), according to the manufacturer’s definition. To allow for a comparison under identical conditions, each case was reconstructed using a HU kernel with the image characteristic “normal”. This setting was identified as being sufficient, when quantitative analyses are desired [6].

*Research supported by the Federal Ministry of Education and Research in Germany within the Research Campus *STIMULATE* under grant number 13GW0095A and by the European Regional Development Fund under the operation number ‘ZS /2016/04/78123’ (project nr.: 5244003000) as part of the initiative “Sachsen-Anhalt WISSENSCHAFT Schwerpunkte”.

P. Berg, S. Voß and G. Janiga are with the Department of Fluid Dynamics and Technical Flows and the Research campus *STIMULATE*, University of Magdeburg, 39106 Magdeburg, Germany (phone: +49-391-67-181-95; fax: +49-391-67-128-40; e-mail: philipp.berg@ovgu.de, janiga@ovgu.de).

L. Radtke is with the Chair in Healthcare Telematics and Medical Engineering and the Research campus *STIMULATE*, University of Magdeburg, 39106 Magdeburg, Germany (e-mail: livia.radtke@st.ovgu.de).

S. Serowy and O. Beuing are with the Department of Neuroradiology, University Hospital Magdeburg, 39127 Magdeburg, Germany (e-mail: steffen.serowy@med.ovgu.de, oliver.beuing@med.ovgu.de).

B. Preim and S. Saalfeld are with the Department of Visualization and the Research campus *STIMULATE*, University of Magdeburg, 39106 Magdeburg, Germany (e-mail: bernhard@isg.cs.uni-magdeburg.de sylvia.saalfeld@ovgu.de).

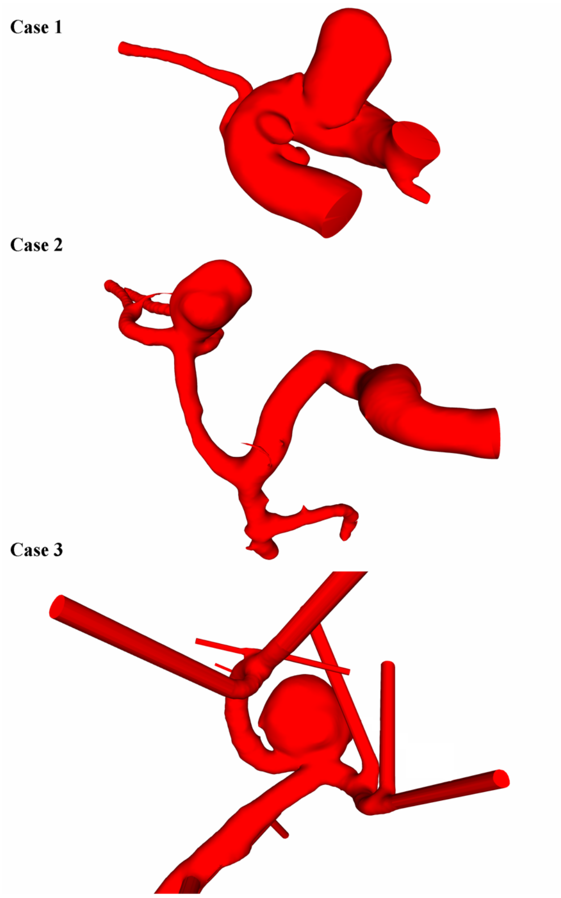

Figure 1. Illustration of the considered patient-specific aneurysms, reconstructed using the highest spatial resoltion ($\Delta x_s = 0.1$ mm); Case 1 (top), Case 2 (center), Case 3 (bottom)

C. Vascular Segmentations

The vascular segmentation was carried out using a clinical research prototype. This prototype enables a very fast generation of three-dimensional vessel surfaces within a few minutes. Hence, it is clinically applicable and was validated in a former study [8]. To ensure developed flow condition within the hemodynamic simulations, in- and outflow areas were extruded in normal direction. As illustrated in Fig. 1, the considered cases are shown. It needs to be mentioned that no modification, such as manual removing of artifacts (e.g., melted vessels or holes in the surfaces), was performed. Hence, only the reconstruction voxel sizes varied and all other working steps were kept constant.

D. Hemodynamic Simulations

Based on the nine segmentation results, time-dependent blood flow simulations using computational fluid dynamics (CFD) were performed with STAR-CCM+ 11.06 (Siemens Product Lifecycle Management Software Inc., Plano, TX, USA). Before the actual computations, the same software was used for spatial dicretization of all simulation domains. A base size of 0.08 mm and three prism layers resulted in a number of polyhedral and prismatic elements ranging from 1.6 million to 3.4 million. For the unsteady simulations, inflow waveforms acquired in a healthy volunteer using 7T phase-contrast magnetic resonance imaging were applied [9]. Further, rigid vessel walls were assumed and zero-pressure outlet boundary conditions were applied at each distal cross-sectional area. Blood was treated as laminar, incompressible (ρ=1055 kg/m^3) and Newtonian (η=4 mPa·s) fluid. A time step size of Δt = 1E-3 s was defined and solutions were assumed to be converged, when residuals for continuity and all three velocity components decreased below 1E-5. Three cardiac cycles were calculated in order to obtain a period solution, while only the last cycle was used for analyses.

E. Analysis

To evaluate potential differences due to the choice of reconstruction voxel size, several morphological as well as hemodynamic metrics were calculated. For the analysis of the segmented geometries, aneurysm surface area A_a, aneurysm volumes V_a and aneurysm ostium areas A_o were considered. Furthermore, the complexity of each aneurysm shape was characterized using the ellipticity index (EI). Equation (1) contains the corresponding definition based on [10]:

$$EI = 1 - (18\pi)^{1/3} \frac{{V_{CH}}^{2/3}}{S_{CH}} \tag{1}$$

where V_{CH} and S_{CH} are the volume and surface area of the convex hull, respectively.

A deviation from the spherical shape is expressed using the nonsphericity index (NSI), which considers the actual aneurysm volume and surface area (2).

$$NSI = 1 - (18\pi)^{1/3} \frac{V^{2/3}}{S} \tag{2}$$

The final morphological parameter used within this analysis is the undulation index (UI). Here, the ratio of aneurysm volume and the volume of the convex hull was considered (3).

$$UI = 1 - (V/V_{CH}) \tag{3}$$

In addition to the geometric analysis, relevant hemodynamic parameters were compared. In this regard, spatial and temporal averaged wall shear stresses (AWSS) were calculated over the cardiac cycle T (4).

$$AWSS = 1/T \int_0^T |wss| dt \tag{4}$$

To account for dimensionless metrics that characterize the shear intensity on each aneurysm surface, shear concentrations indices (SCI) were computed based on the total viscous shear forces F_h and F_a computed over the area of high WSS (A_h) and the entire aneurysm (A_a) (5).

$$SCI = \frac{(F_h \,/\, F_a)}{(A_h \,/\, A_a)} \tag{5}$$

Finally, the flow situation is measured using the inflow concentration index (ICI). Here, the flow rate into the aneurysm Q_{in}, the flow rate in the parent artery Q_v, the ostium area of the aneurysm A_o and the inflow area through the ostium A_{in}, respectively, were used.

$$ICI = \frac{(Q_{in} \,/\, Q_v)}{(A_{in} \,/\, A_o)} \tag{6}$$

Equations (5) and (6) are based on the formulation by Cebral et al. [11].

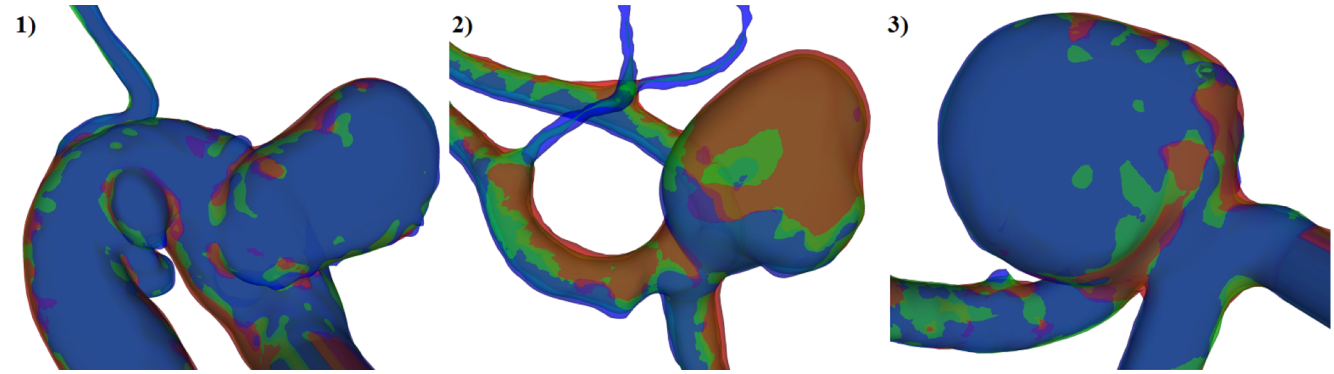

Figure 2. Illustration of the intracranial aneurysm surfaces (Case 1-3) reconstructed using different voxel sizes: “small” ($\Delta x_s = 0.1$ mm, blue), “medium” ($\Delta x_m = 0.3$ mm, green) and “full” ($\Delta x_f = 0.5$ mm, red)

III. Results

A. Morphology

As illustrated in Fig. 2, the effect of different voxel sizes becomes visible. Overall, the three-dimensional segmentations are in a good agreement and the aneurysms appear to be reconstructed almost identical. However, it can be noticed that especially the ostia of the aneurysms experience deviations. While the best resolution enables a sharp transition from the parent vessels to the malformations, lower resolutions (e.g., 0.5 mm voxel size) lead to inaccurate neck representations. Furthermore, small perforators and side branches such as the ophthalmic artery are not captured by the highest voxel size (see Fig. 2, Case 1). Hence, depending on the research question, this effect needs to be respected.

Beside the qualitative observations, Table 1 quantifies relevant morphological parameters for each dataset. The values confirm that only small differences occur regarding the aneurysm surface area and volume, respectively. However, differences with respect to the ostium area are up to 10%, which is not negligible. The same trends are observed for the shape parameters. Although a very good agreement was obtained for EI, clearer differences occur for NSI and UI, respectively (15% and 39%).

TABLE I. Morphological parameters of the different cases considering three voxel sizes (F-full, M-medium, S-small)

Morph. parameter	Case 1			Case 2			Case 3		
	F	***M***	***S***	***F***	***M***	***S***	***F***	***M***	***S***
A_a [mm^2]	155.975	156.245	157.859	150.964	149.435	149.034	188.149	186.139	188.963
V_a [mm^3]	210.713	207.85	205.423	176.183	170.417	165.695	262.655	252.541	246.98
A_o [mm^2]	31.064	29.444	27.941	10.704	9.629	8.721	19	17.442	15.626
EI [-]	0.255	0.256	0.255	0.243	0.244	0.246	0.227	0.23	0.234
NSI [-]	0.129	0.138	0.153	0.201	0.21	0.223	0.163	0.176	0.2
UI [-]	0.05	0.047	0.059	0.035	0.045	0.059	0.03	0.045	0.052

B. Hemodynamics

The evaluation of time-dependent blood flow simulations reveals clear qualitative differences of the resulting wall shear stresses. As shown in Fig. 3, similar stresses are predicted at the parent vessels. However, with increasing voxel size resolution, improved description of the WSS pattern on the aneurysm sac becomes possible.

In addition, the geometrical deviations lead to quantitative variabilities of the hemodynamic parameters. Especially those that are sensitive to wall modifications (e.g., wall shear stresses) experience clear variations (see Table 2). Here, the analysis reveals that deviations of more than 30% can occur (e.g., for ICI), depending on the considered voxel size.

TABLE II. Hemodynamic parameters of the different cases considering three voxel sizes (F-full, M-medium, S-small)

Hemodyn. parameter	Case 1			Case 2			Case 3		
	F	***M***	***S***	***F***	***M***	***S***	***F***	***M***	***S***
AWSS [Pa]	6.99	7.502	7.927	1.572	1.915	1.798	3.574	3.395	3.14
nWSS [-]	0.518	0.532	0.597	0.22	0.282	0.255	0.68	0.671	0.62
SCI [-]	6.47	6.835	6.84	2.08	2.332	2.157	4.3	4.544	4.279
ICI	0.81	0.925	0.978	0.641	0.512	0.545	1.277	1.207	1.188

IV. Discussion

Advanced computational studies based on morphological and hemodynamic computations are increasingly used to assist physicians regarding therapy planning. However, since several interdisciplinary steps are involved, until reliable results can be obtained, clinical acceptance remains limited. To improve this situation, transparent analysis of original data (e.g., due to image acquisition) is needed. Hence, the effect of different reconstruction voxel sizes is evaluated.

The results of this study demonstrate that quantitative differences with respect to morphology and hemodynamics occur based on the choice of reconstruction voxel size. One example is a voxel size-dependent reconstruction of the aneurysm ostium, which is an important metric for physicians, since the neck is used for therapy planning. Additionally, several studies containing large number of aneurysms derive conclusions with respect to rupture risk assessment based on existing shear stress patterns and associated shear indices. Here, careful examination of pre-simulative working steps would be desirable in order to avoid error-prone CFD results.

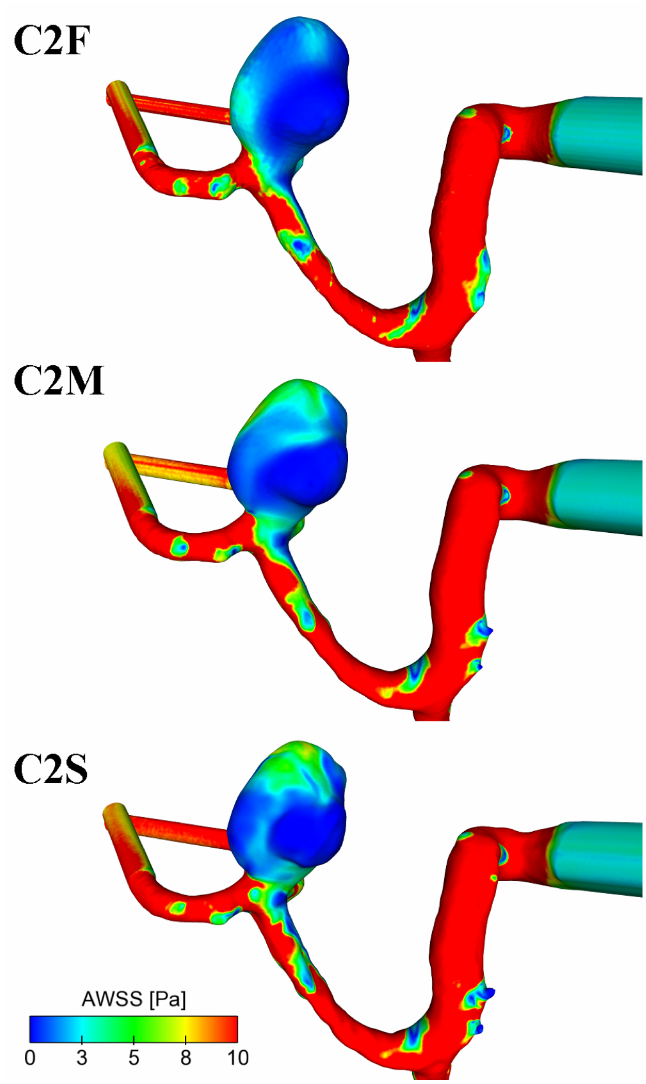

Figure 3. Representative time-averaged wall shear stresses (AWSS) for Case 2 based on three voxel sizes: full (top), medium (center), small (bottom)

Since this computational study includes several working steps, it has clear limitations. Firstly, only datasets acquired using 3DRA were considered. However, other imaging modalities such as CTA or MRA are used to evaluate intracranial aneurysms. Nevertheless, this study focused on the gold-standard with respect to spatial resolution. Secondly, hemodynamic simulations require simplified boundary conditions due to the lack of individual flow information and the absence of precise in-vivo measurement techniques. Nonetheless, all cases were simulated using identical CFD conditions, which enables comparability. Thirdly, the number of aneurysms is small. Hence, findings cannot be generalized and further investigations containing a higher number of cases is required. However, this pilot study enables an awareness of the effects of early image processing.

Future work contains an increasing of the number of patients, which also allows for a categorization with respect to location. Since the parent vessels of more distal aneurysms (e.g., at the anterior communicating artery) possess clearly smaller calibers compared to aneurysms at the internal carotid artery, different effects of the reconstruction voxel size are expected.

V. Conclusion

The choice of reconstruction voxel size based on 3DRA image data clearly influences advanced morphological as well hemodynamic analyses of intracranial aneurysms. Hence, if precise studies with respect to rupture risk assessment or treatment optimization are desired, careful reconstruction is advised to avoid unnecessary errors.

Acknowledgment

The authors warmly acknowledge Dr. Thomas Redel (Siemens Healthineers, Erlangen, Germany) for his support regarding the CFD research prototype.

Disclaimer

The concepts and information presented in this paper are based on research and are not commercially available.

References

[1] G.J. Rinkel, M. Djibuti, A. Algra, and J. van Gijn, "Prevalence and risk of rupture of intracranial aneurysms: a systematic review", *Stroke,* 29, pp. 251–256, 1998

[2] K. Valen-Sendstad, M. Piccinelli, R. KrishnankuttyRema, and D.A. Steinman, „Estimation of inlet flow rates for image-based aneurysm CFD models: where and how to begin?", *Ann. Biomed. Eng.,* 43, pp. 1422–1431, 2015

[3] C. Chnafa, O. Brina, V.M. Pereira, and D.A. Steinman, "Better than nothing: a rational approach for minimizing the impact of outflow strategy on cerebrovascular simulations", *Am. J. Neuroradiol.,* 2017.

[4] H.G. Morales, I. Larrabide, A.J. Geers, M.L. Aguilar, and A.F. Frangi, "Newtonian and non-Newtonian blood flow in coiled cerebral aneurysms", *J. Biomech.,* 46, pp. 2158–2164, 2013

[5] P. Berg, C. Roloff, O. Beuing, S. Voß et al., and G. Janiga, "The computational fluid dynamics rupture challenge 2013-phase II: variability of hemodynamic simulations in two intracranial aneurysms", *J. Biomech. Eng.*, 137(12), 121008/1-13, 2015

[6] P. Berg, S. Saalfeld, S. Voß, T. Redel, B. Preim, G. Janiga, and O. Beuing, "Does the DSA reconstruction kernel affect hemodynamic predictions in intracranial aneurysms? An analysis of geometry and blood flow variations", *J. NeuroIntervent. Surg*., 0, pp. 1–7. doi:10.1136/neurintsurg-2017-012996, 2017

[7] A. Lauric, J.E. Hippelheuser, and A.M. Malek, "Critical role of angiographic acquisition modality and reconstruction on morphometric and haemodynamic analysis of intracranial aneurysms", *J. NeuroIntervent. Surg*., 2018

[8] P. Berg, S. Voß, M. Becker, S. Serowy, T. Redel, G. Janiga, S. Skalej, and O. Beuing, "Bringing hemodynamic simulations closer to the clinics: a CFD prototype study for intracranial aneurysms", In: *IEEE Engineering in Medicine and Biology Society (EMBC'16)*, Orlando, USA, pp. 3302-3305, DOI: 10.1109/EMBC.2016.7591434, 2016

[9] P. Berg, D. Stucht, G. Janiga, O. Beuing, O. Speck, and D. Thévenin, "Cerebral blood flow in a healthy Circle of Willis and two intracranial aneurysms: computational fluid dynamics versus four-dimensional phase-contrast magnetic resonance imaging", *J. Biomech. Eng,* 136, 2014

[10] M.L. Raghavan, B. Ma, R.E. Harbaugh, „Quantified aneurysm shape and rupture risk", *J. Neurosurg.*, 102, pp. 355–362, 2005

[11] J.R. Cebral, F. Mut, J. Weir, and C. Putman, "Quantitative characterization of the hemodynamic environment in ruptured and unruptured brain aneurysms", *Am. J. Neuroradiol.,* 32, pp. 145–51, 2011